福 井 大 学 審査
学 位 論 文 [ 博士 (工学) ]

# Mechanism of Electrocatalytic Reduction of Dioxygen with Hemin
## (ヘミンによる酸素の電気化学的触媒還元反応の機構)

平成二十七年九月
李　文 文

# Abstract

The thesis deals with electrochemical reduction of dioxygen with hemin on different kinds of electrodes in different kinds of solutions in order to find functionality of hemin catalysis for dixoygen and its catalytic mechanism. The aim of this research is to investigate the mechanism of reaction, build the reaction model and discuss its application in normal which is based on analysis of the electrochemical reduction currents of dioxygen by hemin with different states on electrode surface in different kinds of solutions. This study was performed to improve understanding of the kinetic mechanism in heterogeneous catalysts for oxygen reduction reaction(ORR).

Chapter 3 is devoted to examining irreversibility of catalytic reduction of dioxygen by dissolved hemin. According to cyclic voltammogram(CV), peak currents in deaerated hemin solution is diffusion controlled, whereas that in aerated solution is represented as a sum of the diffusion current and a surface wave. The results mean that the catalytic current presents and it is caused by hemin incorporated with dioxygen. The calculated value of adsorption density is close to accepted values of the monolayer adsorption as well as reported values of adsorbed hemin. The agreement indicates that the catalytic reduction of dioxygen should occur at glassy carbon electrode surface by hemin in adsorbed species state in dimethyl sulfoxide (DMSO). The voltammograms figures showed that the catalytic current cannot keep a steady state even if dioxygen is supplied to the electrode by diffusion or convention. Actually the reaction will be interrupted if the adsorbed species is not dissolved at the oxidation at 0.3 V. In other words the electrode surface is not renewed sufficiently for the catalytic reaction. In order to keep the catalysis for a long time, it is necessary to remove the adsorbed species. Consequently, the catalysis is not suitable for an alternative to precious metals in fuel cells.

Chapter 4 is devoted to relationship between electrochemical catalysis and the

generation of a dioxygen adduct of hemin. Two different conditions were performed to study the inner link of currents from hemin-coated electrode and dissolved hemin. At the hemin-coated electrode is not proportional to the amount of adsorbed hemin but is controlled by dioxygen because the hemin film is superfluous for dioxygen relatively on electrode surface. The catalytic current is controlled by diffusion of dioxygen, associated with the successive two-electron transfer reaction. The hemin-coated electrode can be used quantitative determination of dioxygen without rigorous control of the amount of hemin; In solution with dissolved hemin, the dioxygen adduct of hemin plays a role of an intermediate of the catalytic reaction, via the reaction equation: $O_2 + 2hem(Fe^{2+}) \leftrightarrow (hem(Fe^{2+}))_2O_2 \rightarrow O_2^{2-} + 2hem(Fe^{3+})$. Ultraviolet spectrum results supply a lateral confirmation of this reaction.

# Acknowledgements

I would like to sincerely thank Professor Koichi Aoki and Associate Professor Jingyuan Chen who came out on my way to another mountain top of learning and gave me not only the help on school work but also on life in Japan. Without their conscientious guidance, selflessly help and warm encouragement, these works would have not been accomplished possibly. Sometimes you should not see one thing perfunctorily, deeply I think I will profit from their advice in the future in my life. My parents give me life and guide me at the front of life stage, the teachers stand by me in school life.

I want to show my respect Associate Professor Dr. Toyohiko. He always pays much attention on our experiments and do care about our safety in experimental procedure. He is one person, who shows much more respect on rules rather than human emotion. There are no rules, there are nothing stay forever. In a sense, he is a typical Japanese. He taught me how to be a researcher and gave me a lot of advice in this work too.

I would also express my thanks to Tianbao.Li, Han.Chen, and Chaofu. Zhang. Because of some reasons, I cannot afford my life in Japan at first, with their help I stick to that stage. And I want to thank other members of Aoki Research Group for their warm helps with my study and daily life in Japan.

Finally heartful gratitude goes to my dear parents. Without their support and contribution, I will never go this way at leisure. Although when got the call from father, his first word was always like this: “Do you need more money”, I know that he is always a great father who is not good at expressing his deep emotion. And I want to say thanks to my younger sister,

who got married in this year.

Actually, I would like to say thank you to my ex-girlfriend who stays with me, not body but spirit, for 3 years. Wish her all the best.

Sincerely Yours,

Wenwen Li

Department of Applied Physics
University of Fukui, Japan

11/17/2014

# Contents

# Chapter 4

## Relationship between electrochemical catalysis and the carriage of dioxygen by hemin



# Chapter 5

## Conclusion

# Chapter 1

## Introduction

### 1.1 Property of hemin

Hemin($C_{34}H_{32}ClFeN_4O_4$) is one chemical substance which is similar with the key reaction structure of enzymes, such as cytochrome, hemoglobin and other hemoproteins. It contained an iron(III) ion which is held in a heterocyclic ring, known as a porphyrin. The structure of a hemin group is showed in scheme 1[1].

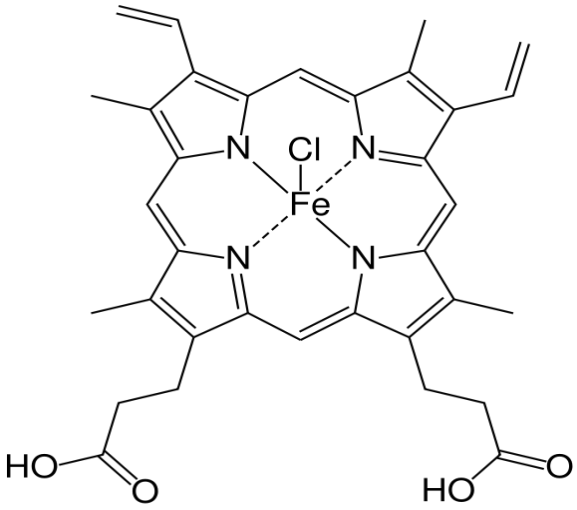


Scheme 1 structure of hemin group

Hemin is a macromolecule(molar mass 651.94g/mol) with high hydrophobicity and low solubility in neutral and acidic aqueous solution, but it can dissolve in alkaline solution and some organic solvent.

### 1.2 Research on hemin

Chemical modification is an interesting and useful way to help scientists obtain functional materials to extend research field. Among modifications, the modification of electrode surface by using specific substance is an important application. A number of researchers with their co-workers have investigated this field through the study of iron porphyrins, in these studies, hemin acted as an important role. Ason, Tsuchida and co-workers have incorporated certain iron porphyrins into polymer matrices while working in aqueous media[2-5]. Kadish and others have chosen iron porphyrin in non-aqueous media[6-8]. Others have exmined the possibility of attaching polymer bound porphyrins to crystalline electrode surfaces[9]. These workers are aim at mixing hemin with other polymer and immobilize them on electrodes with different materials (grapheme[10] or multi-walled carbon nanotubes, for example) or different ways to treat the mixed materials (controlling the temperature to modify the electrode[11]), and testing their sensibilities for the dioxygen or superoxide[12] or other species and stability of modified electrodes. Among these studies, direct evidence for catalysis of oxygen by some iron porphyrin system has been confirmed [13-16].

In recent years, some specific organic molecules were used for enhancing the electronic properties of semiconductors. This method has attracted much vision because of their high stability and variety [17]. Special attention has been focused on metalloporphyins, especially hemin, which may display tunable cooperative interactions very attractive for applications in oxidation chemistry, catalysis, and molecular recognition[18-19].

## 1.3 Application of hemin

Hemin, with similar structure of heme unites in myglobin and hemoglobin, is substitution in some biological and biochemical studies：the hemin has superior

chemical reactivities when coupled with specific protein environments as found in nature. And it is also very important in electrochemical research. Hemin has become one interesting compound capable of catalysis in ORR and valuable model for investigating electron transfer in hemoproteins [20]. Because of its relevant role in oxygen and hydrogen peroxide reduction [21-22] or in nitric oxide (NO) physiology[23], hemin seems to be an ideal molecule to design new oxygen[24]/NO sensors[25-26]. A variety of strategies have been employed to produce chemically modified electrodes to study the electrochemical reduction of dioxygen by hemin[27-33]. Some of the researchers focused on the modification of hemin and its polymer on the electrode surface. They are interested in mixing hemin with other species(such as carbon paste or carbon nano tube(CNT)) to strengthen property. In these works, covalent bonding, adsorption and electrochemical polymerization of hemin have been employed to modify the carbon based or metal electrode surfaces. The mixture-modified electrodes were used as sensors for different species. For example, Arifuku reported an electrochemical study concerning the catalytic dioxygen reduction on glassy carbon electrodes modified by covalent bonding of hemin[34]. Otherwise, many systems, using hemin or hemoglobin as mediator for catalytic reduction of hydrogen peroxide or dioxygen, were reported[35-39].

Currently, materials of platinum-based precious metals are considered as the only functional catalytic material for fuel cells. Because of well-known economic reasons, iron porphyrins and phthalocyanines have been studied for ORR for alternatives due to their high catalytic activity [40-42]. Researchers want to extend its application on fuel cells. Recently, some researchers have found that heat-treated porphyrins and phthalocyanines improved their catalytic activity and stability [43-45]. In addition, several groups have reported that heat-treated carbon materials containing nitrogen have catalytic activity for the ORR[46-49]. Liangetal found good ORR catalytic activity of hemin after heat-treating the hemin supported on carbon black[50].

## 1.4 Motivation

There are various of directions to study the catalysis of hemin for dioxygen(or nitric oxide or other species). The catalysis of dioxygen by hemin has been examined by William R.Heineman and his co-workers[51] as a the pioneer of voltammetric catalysis of hemin and unfortunately, the absolute values of the current have not been discussed which include possibilities of several rate determining steps will lead to comprehend the reaction process on carbon electrode.

Based on research status, we will challenge the electrocatalytic and chemical behavior of hemin with dioxygen.

## 1.5 Aim of thesis

The aim of this research is to obtain the reaction mechanism of hemin with dioxygen, build the reaction model and discuss its applications.

# Chapter 2

## Experimental section

### 2.1 Chemicals

Hemin (Chlorohemin, > 95%) was purchased from Tokyo Chemical Industry Co. Ltd (Tokyo, Japan). It was weighed after it became at a room temperature in order to avoid mixing with water.

Tetrabutylammonium Perchlorate ($C_{16}H_{36}ClNO_4$) was supplied by Tokyo Chemical Industry Co. Ltd (Tokyo, Japan).

Dimethylsulfoxide $(CH_3)_2SO$ was bought from Wako Pure Chemical Industry. Ltd (Osaka,Japan). DMSO was distilled under reduced pressure and dried by means of molecular sieves.

Ferrocene ($C_5H_3FeC_5H_5$) and Acteone ($CH_3CO$) were got from Wako Pure Chemical Industry. Ltd (Osaka, Japan).

Nitrogen gas was provided by Uno Gas Industry. Ltd

Oxygen gas was provided by Uno Gas Industry. Ltd

### 2.2 Electrode preparation

Platinum(Pt) electrode was polished with silicon carbide polishing paper (DTC, grade 1200) then 1μm and 0.3μm alumina(Buehler) and rinsed througly with deionized water and eventually dried. This polishing leads to a mirror-like surface for glassy carbon electrodes and low surface roughness [52].

Glassy carbon working electrodes (GC, 3.0mm in diameter) sealed by non-conducting rubber and connected to copper wires. According to different

experiments, GC electrodes was barely or modified by 0.03ml hemin-only solution (solvent is DMSO) with different concentrations. The procedure of polishing GC electrodes are same as Pt electrode. The cleaned GC electrode was modified with hemin which was dissolved in DMSO, and dried at 60 degree centigrade for 4 hours in vacuum drying oven. All of modified electrodes are made by following this procedure.

## 2.3 Electrochemical measurements and installations

All of experiments were performed in a three-electrode system including one Pt wire auxiliary electrode, a $Ag/Ag^{+}$ (0.01 M $AgNO_3$, M = mol $dm^{-3}$) reference electrode and a working electrode. The working electrodes were the glassy carbon electrode 3 mm in diameter, the platinum disk electrode 1.6 mm in diameter and the gold disk electrode 1.6 mm in diameter. They were commercial available (BAS, Tokyo). A small disk platinum electrode, 0.1 mm in diameter, was home-made, coated with glass. A Pt mesh (The Nilaco Co. Ltd, Japan) working electrode with 50% transmittance was placed in a spectrophotometric cell (0.4 mm light path length) and used for spectroelectrochemical measurements. The other two electrodes for UV measurements were Ag/Ag+ electrode and Pt coil. A compactstat iviumtat (Ivium Technologies De Zaale 11 5612 AJ Eindhoven, Netherlands) combined with a three-electrode system was used for all electrochemical experiments. Two Pt disk working electrode(1.6 mm in diameter and 0.1 mm in diater) and GC,3.0 mm in diameter, were used as working electrodes respectively, the Ag/Ag+ electrode was used as reference electrode and Pt coil was used as counter electrode in three-electrode system as showed by scheme 2.

A UV/Vis spectrophotometer (JASCO V-570 (JASCO Corporation)) was used in the ultraviolet adsorption spectrometry(showed in scheme 2).

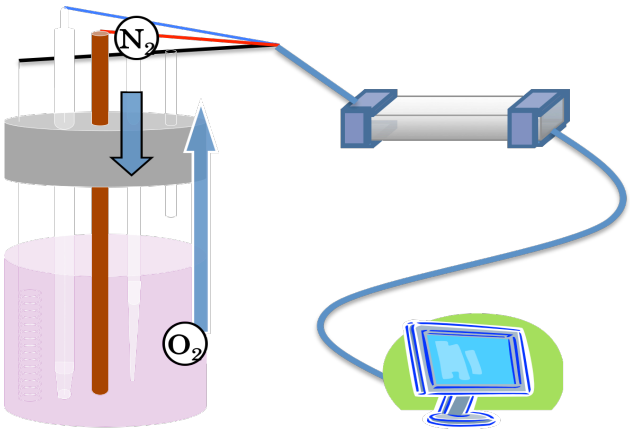


Scheme 2. Schematic diagram of experimental facility

# Chapter 3

## Irreversibility of catalytic reduction of dioxygen by dissolved hemin

### 3.1. Introduction

Cobalt phthalocyanine has been demonstrated to work as electrocatalysis of the oxygen reduction reaction (ORR) in alkaline media by Jasinski for the first time [53]. Since then, the catalytic activity of metal porphyrins has been explored as alternatives of non-precious metal catalyst for ORR. Especially hemin, a natural porphyrinatoiron complex, has been able to reduce catalytically dioxygen and hydrogen peroxide at carbon paste electrodes [54-56]. Hemin-modified carbon fiber electrodes can also reduce dioxygen to water and hydrogen peroxide, depending on solvents [57]. The number of electrons transferred at hemin-coated glassy carbon electrodes varies with pH; a one-step four-electron reduction at pH < 11 and two successive steps at pH > 12 [58]. Heat treatment of hemin-modified carbon electrodes has enhanced the catalytic efficiency of ORR close to that of platinum electrodes [59]. Functional groups on the porphyrin periphery play a part in the electrocatalytic ORR, reportedly [60]. Catalytic performance has been improved by use of hemin/graphite felt composite electrodes [61], by immobilization of hemin on chemically converted graphene [62] and carbon nanotubes [63-65], by electrostatic binding of hemin on latex particles [66], by enhancing porosity of adsorbed layers [67,68], by heating the hemin-modified electrodes [59,69-71], and by immobilization of hemin into proteins [72]. Catalytic activity of hemin has been found for reductions of NO [73,74], mercuric ion [75], antimalarial drug [76], nitrite [64,65], and hydroquinone [77].

The well-known electrochemical, catalytic reaction is exemplified by the Fenton reaction, in which electrochemically generated ferrous ion is oxidized to ferric ion by

hydrogen peroxide [78], i.e.

$Fe^{3+} + e^- \rightarrow Fe^{2+}$ (1)

$Fe^{2+} + H_2O_2 \rightarrow Fe^{3+} + OH^- + OH\cdot$ ($k$: reaction rate constant) (2)

Expressions for the catalytic current by linear sweep voltammetry have been derived on the assumption of the mixed control of reaction (2) with diffusion of the soluble species [79]. The catalytic current at a large value of the reaction rate $k[Fe^{2+}][H_2O_2]$ is independent of scan rates, $v$, and is controlled by diffusion of $H_2O_2$. In contrast, the current at a very small value of the rate is proportional to $v^{1/2}$. As a result, the current varies generally with $v^p$ for $0 < p < 0.5$. This relation is, however, different from the voltammetric results ($p > 0.5$) of reduction of dioxygen with hemin although the model of reactions (1) and (2) has been applied to the analysis [56,58,60,61]. The other available model is the catalytic reaction of soluble species with the redox species adsorbed on an electrode [80]. This has not been applied to experimental results of hemin, to our knowledge, probably because application of the theoretical expressions needs detailed dependence on concentrations and scan rates. Another model used is for the preceding reaction at a rotating disk electrode [62,67,69]. It is obviously not suitable for explanations of the catalytic reaction.

The catalysis of dioxygen by hemin can be applied to fuel cells if current flows under the steady state in dioxygen-rich solutions. The steady-state currents have been observed at rotating disk electrodes [58,62,67,69]. It is not clear, however, whether the currents are a purely catalytic component or include direct reaction by hydrodynamic transport of dioxygen. In order to discern the catalytic component from the direct mass transport reactions, it is necessary select conditions under which the reduction potential of hemin is much more positive than that of dioxygen. One technique is to use dimethylsulfoxide (DMSO) in which the potential difference is over 0.4 V [81]. Then we may examine time-variation of the catalytic currents in details. This report deals with time-dependence of the catalytic currents of dioxygen by hemin in DMSO, varying

concentrations of dioxygen and hemin. The catalytic current will be demonstrated to be decaying current by adsorption process [82,83], rather than under the steady state.

## 3.2. Experimental

All the chemicals were of analytical grade. Hemin (Wako) with nominal 97 % purity was stored in a refrigerator. It was weighed after it became at a room temperature in order to avoid mixing with water. DMSO was distilled under reduced pressure and dried by means of molecular sieves.

A potentiostat used was Compactstat (Ivium, Netherlands). All electrochemical experiments were performed in a three-electrode cell including a Pt wire auxiliary electrode, a $Ag/Ag^{+}$(0.01 M $AgNO_3$, M = mol $dm^{-3}$) reference electrode and a working electrode. The working electrodes were the glassy carbon electrode 3 mm in diameter, the platinum disk electrode 1.6 mm in diameter and the gold disk electrode 1.6 mm in diameter. They were commercial available (BAS, Tokyo). A small disk platinum electrode, 0.1 mm in diameter, was home-made, coated with glass.

Spectro-electrochemical measurements was made with V-570 UV/VIS/NIR Spectrophotometer (Jasco, Japan). The spectro-electrochemical cell had a thin layer cell made of quartz 0.47 mm thick, into which the Pt mesh 0.076×50×10 $mm^3$ with the density 80 was inserted.

## 3.3. Results and Discussion

### 3.3.1 Reaction model of dissolved hemin

If there is no hemin in Dimethyl sulfoxide solution, there is no reaction can be observed from Fig.1(a), it means the electrolyte will not affect the reaction. When

hemin was added into the dimethyl sulfoxide solution, we can observe the reaction from Fig.1(b).

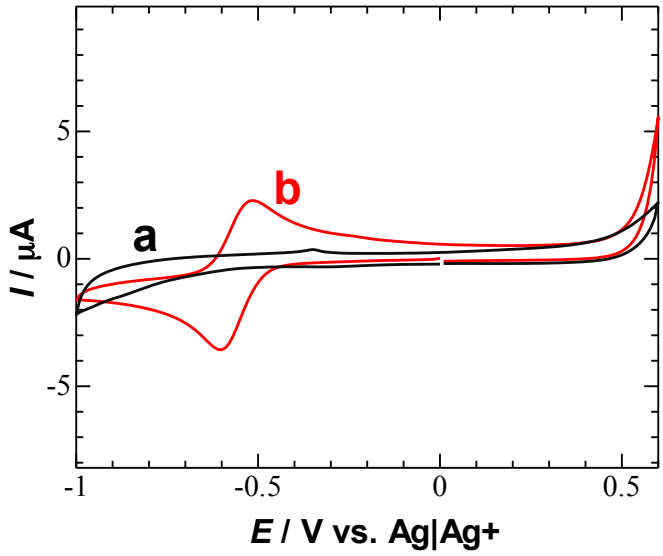


**Figure.1.** Cyclic voltammograms in (a) deaerated 0.15 M $TBAClO_4$ + DMSO solution and (b) deaerated 0.15 M $TBAClO_4$ + 0.33 mM hemin + DMSO solution, for $v$ = 0.1 V $s^{-1}$ at the GC electrode.

Because there is not any other reactant else in DMSO expect Tetrabutylammonium Perchlorate and we also have known that the Tetrabutylammonium Perchlorate will not affect the reaction, so there is no doubt that the peaks which are -0.55 V and -0.65 V are responsible for hemin. It is redox and reversible reaction of iron ion in hemin species as follows:

Reduction reaction at -0.65 V :

$HmFe^{3+} + e^- \rightarrow HmFe^{2+}$

Oxidation reaction at -0.55 V :

$HmFe^{2+} - e^- \rightarrow HmFe^{3+}$

The voltammogram in hemin-included deaerated DMSO solution showed a couple of redox waves approximately at -0.7 V in Fig. 2(a). The other couple at -1.7 V (not

shown here) is not related with the present discussion. Since the cathodic and the anodic peak currents were proportional to concentrations of hemin less than 3 mM, the wave should be caused by the reduction of hemin. The voltammograms did not vary with iterative scans. The cathodic peak current was proportional to the square roots of scan rates, $v$, as shown in Fig. 3(a), and hence it should be controlled by diffusion of hemin. Concentration of electroactive hemin is smaller than that prepared by weight [84]. In order to determine the concentration accurately, we applied the method of the combinational use of a small electrode (0.1 mm in diameter) and a regular electrode (1.6 mm in diameter) [84]. This technique allows us to determine concentrations without knowing a value of the diffusion coefficient. The reduction peak currents at the 1.6 mm electrode were proportional to $v^{1/2}$ for $0.01 < v < 0.2$ V $s^{-1}$. In contrast, those at the 0.1 mm electrode showed a linear relation with $v^{1/2}$ with an intercept. Taking the ratio of the slope of the former plot to the intercept of the latter plot [84], we evaluated the concentration to be 0.40 mM, which was smaller than that estimated from the weight (0.6 mM). The diffusion coefficient was evaluated to be $3.3\times10^{-6}$ $cm^2$ $s^{-1}$ in DMSO.

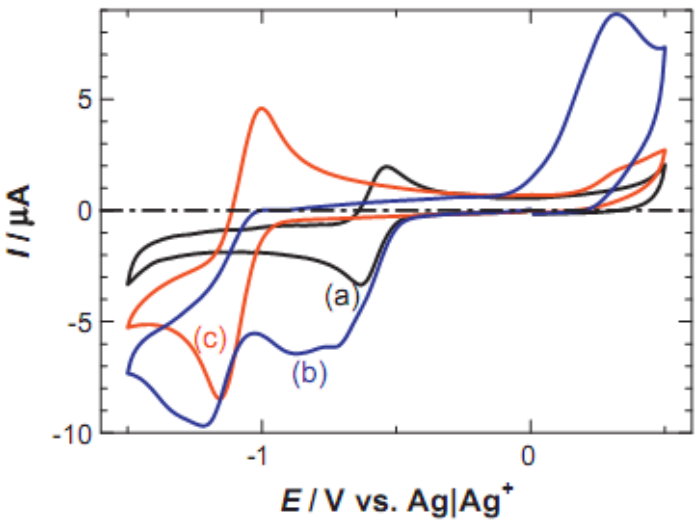


**Figure.2.** Cyclic voltammograms in (a) deaerated and (b) deaerated 0.15 M $TBAClO_4$ + 0.33 mM hemin + DMSO solution, and in (c) aerated 0.15 M $TBAClO_4$ + DMSO solution for $v = 0.1$ V $s^{-1}$ at the GC electrode.

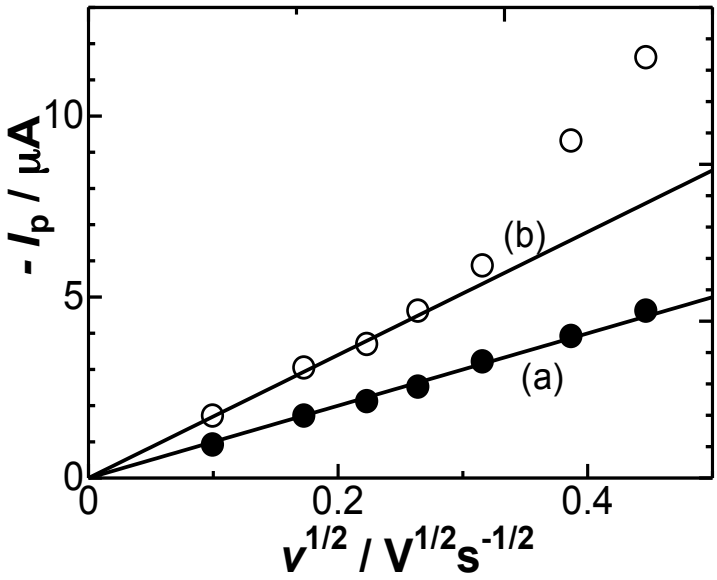


**Figure.3.** Scan rate dependence of the cathodic peak current at ca. -0.7 V in (a) the deaerated and (b) the aerated 0.15 M $TBAClO_4$ + 0.40 mM hemin + DMSO solution at the GC electrode. The inset is the dependence of the difference between (a) and (b) on *v*

When the hemin solution contained air, three cathodic waves appeared at -0.70 V, -0.9 V and -1.20 V, as shown in Fig. 2(b). The current at the first wave was by 1.5 times larger than the reduction peak of hemin, at the cost of the corresponding anodic current. The voltammogram in aerated solution without hemin had no wave at -0.7 V or -0.9 V but showed the reduction wave at -1.2 V. The wave at -1.2 V can be ascribed to the reduction of dioxygen because the current was proportional to concentrations of dioxygen, as will be shown later. The enhancement of reduction peaks at -0.7 V and -0.9 V should be catalytic current of dioxygen by hemin. The energetic gain of the catalysis is 0.5 V (= -0.7 -(-1.2)) or 48 kJ $mol^{-1}$, close to the bibliographic value [81]. The anodic wave at 0.2 V appeared in the aerated hemin solution when the potential was reversed at either -0.8 V or -1.0 V. Therefore it should be due to the products of the catalytic reactions.

In order to identify the species relevant to the catalytic reaction, we made

spectro-electrochemical measurements at the platinum mesh electrode. Figure 4 shows UV-spectra of (a) deaerated hemin solution when hemin, denoted by hem($Fe^{3+}$), was electrochemically reduced to hem($Fe^{2+}$) at the mesh electrode. The Soret bands appeared at 404 nm and 424 nm for (a) hem($Fe^{3+}$) and (b) hem($Fe^{2+}$), respectively, as are consistent with documented data [81,85-89]. When the hemin solution contained dioxygen (c), the band at 424 increased at the expense of the band at 404 nm. Therefore the reduced hemin should be responsible for the catalysis of dioxygen.

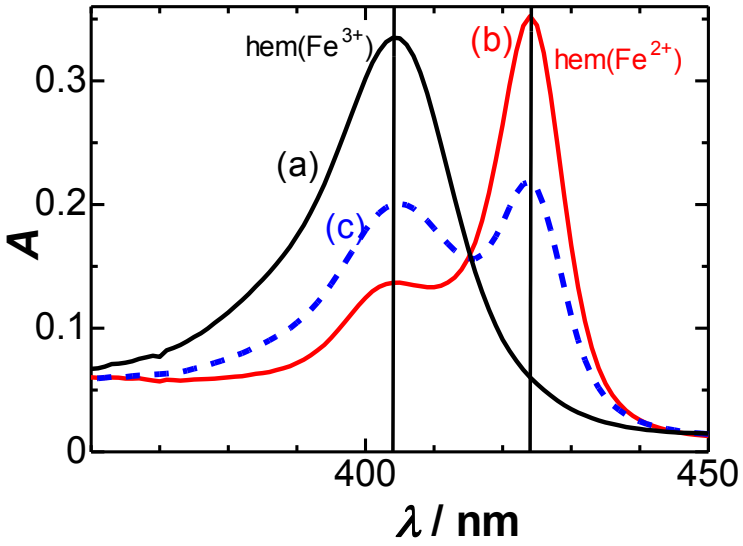


**Figure.4.** UV-vis spectra in (a) the deaerated and (c) the aerated DMSO solutions including 0.033 mM hemin + 0.015 M $TBAClO_4$, and (b) 16 min after -1 V was applied to the Pt mesh electrode in the deaerated solution

The time-variations of the absorbance are shown in Fig. 5 at (A) 404 nm and (B) 424 nm. The concentration of hem($Fe^{3+}$) (at 404 nm) in the deaerated solution decreased with the electrochemical reduction (circles) to generate hem($Fe^{2+}$) (424 nm). When dioxygen is present, hem($Fe^{3+}$) is reproduced with dioxygen by the amount of the concentration of the bold arrow in Fig. 5(A) (triangles), at the cost of hem($Fe^{2+}$) in Fig. 5(B). These variations have reminded electrochemists [56,58,60,61] of the Fenton model of

reaction (1) and (2), i.e.

$$\text{hem}(Fe^{3+}) + e^- \rightarrow \text{hem}(Fe^{2+}) \qquad (3)$$

$$\text{hem}(Fe^{2+}) + O_2 \rightarrow \text{hem}(Fe^{3+}) + O_2^- \text{ (rate constant } k) \qquad (4)$$

On the assumption that hem($Fe^{3+}$) would be generated at the first order reaction rate, we plotted logarithms of the normalized concentration of hem($Fe^{3+}$), i.e. $A$(aerated)/$A$(deaerated) at 404 nm, against the time in Fig. 5(A) on the right ordinate. The plot fell on a line, suggesting the first order reaction with respect to hem($Fe^{3+}$). The value of the slope was 0.0023 $s^{-1}$. Since the reaction rate is expressed by $k$[hem($Fe^{3+}$)][$O_2$], the value of the rate constant $k$ is 9.2 $M^{-1}$ $s^{-1}$ for the concentration (0.5 mM) of the air-saturated dissolved dioxygen at 1 atm. The half-life of the reaction is 5 min (= ln(2)/0.0023 $s^{-1}$). This is too long for the time scale (a few seconds) of the present voltammetry to be observed catalytic currents.

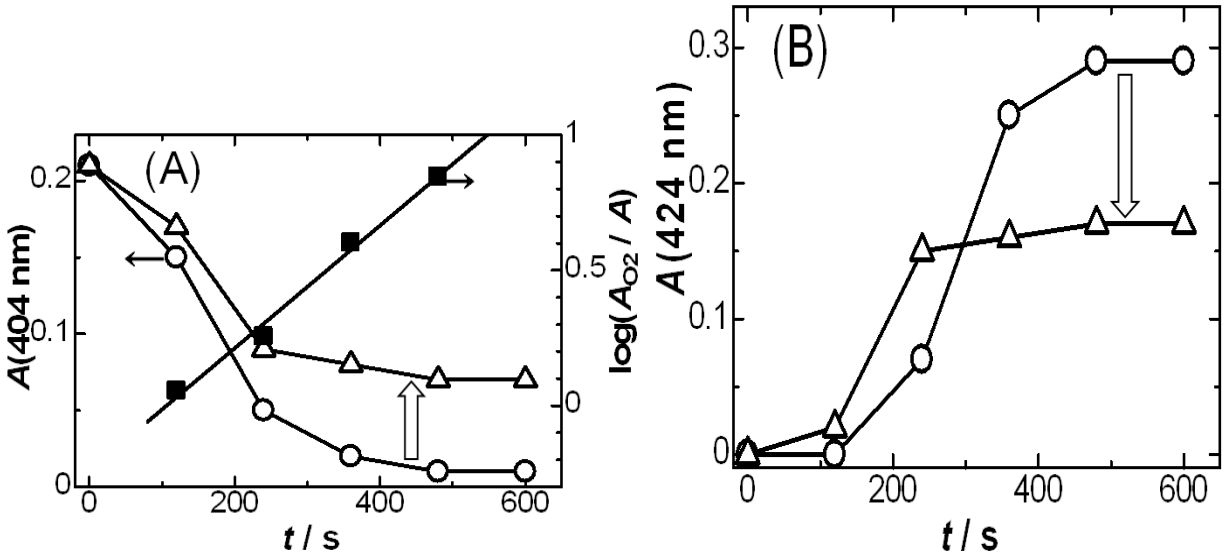


**Figure.5.** Time variation of the absorbance at (A) 404 nm and (B) 424 nm in the (triangles) aerated and the (circles) deaerated DMSO solutions including 0.033 mM hemin + 0.015 M $TBAClO_4$ after -1 V was applied to the Pt mesh electrode. The right ordinate is the logarithm of the absorbance of the aerated solution to that of the time

In order to solve this contradiction, we examined the dependence of the current on the scan rates and concentrations of hemin and dioxygen in detail. Figure 3(b) shows the plot of the catalytic peak current at ca. -0.7 V against $v^{1/2}$. If the catalytic reaction occurs according to the reported mechanism (3) and (4), the current at very slow scan rates must be independent of time or $v$. Quantitatively, the steady-state current density is represented by $Fc^*(kD[O_2])^{1/2}$ for the diffusion coefficient $D$ of fem($Fe^{2+}$) and its bulk concentration $c^*$ [79]. On the other hands, the catalytic current at high scan rates should be proportional to $v^{1/2}$ [79]. The plot in Fig. 3(b) is opposite to the prediction.

We changed the concentration of dioxygen by mixing three aliquots at adequate volume ratios; the deaerated, the air-saturated and the dioxygen-saturated hemin solutions. Figure 6 shows variation of the catalytic currents with the concentration ratios

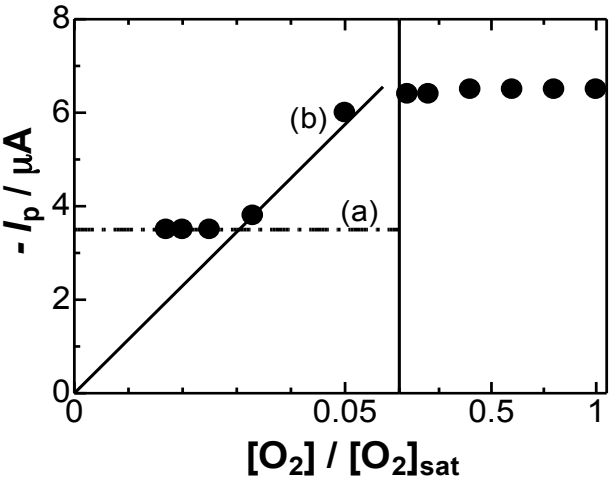


**Figure.6.** Variation of the catalytic peak current at -0.7 V with concentration of dioxygen, obtained for $v$ = 0.1 V $s^{-1}$ at the GC electrode in DMSO solution including 0.4 mM hemin + 0.15 M $TBAClO_4$

to the dioxygen-saturated solution at a given concentration of hemin. The current did not vary with the concentrations less than 0.03 of the dioxygen-saturated concentration (line (a)). The invariance indicates that the current should be controlled by the concentration of hemin. The current at the concentration ratio ranging from 0.03 to 0.06

varied proportionally to the concentration ratio (line (b)). It reached -6.5 μA for the ratio over 0.06. These variations are different from the conventional catalytic current which increases with an increase in concentration of catalyzed species (dioxygen) [79,90] even for the second order reaction [91]. Figure 7 shows plots of the catalytic peak currents against concentrations of hemin, [hemin], in the air-saturated solution. The current without dioxygen is proportional to hemin concentration (a), whereas that with dioxygen increases linearly with the concentration (b) as if the catalysis might occur even at [hemin] = 0, as shown at the intercept of the dashed line.

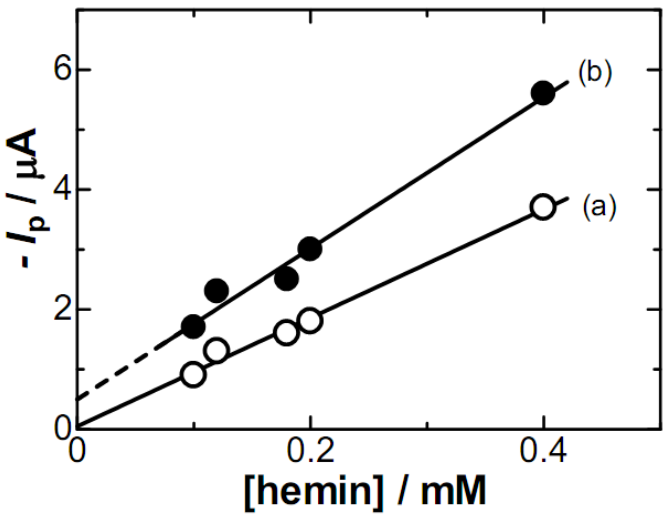


**Figure.7.** Dependence of the peak currents at ca. -0.7 V in (open circles) deaerated and (filled circles) aerated solutions on concentrations of hemin at $v$ = 0.1 V $s^{-1}$

We made iterative, voltammetric runs, between which dioxygen gas was bubbled in the solution. Figure 8 shows dependence of the peak currents (a-c) at -0.7 V for the catalytic current and of those (d) at -1.2 V for the reduction of dioxygen without hemin on the time of the bubbling. The reduction current of dioxygen without hemin increased with the time and reached the saturated value at 900 s, as is in accord with the conventional deaeration process. When solution contained hemin, the catalytic current

increased with the time in the same manner as the increase without hemin before 150 s bubbling. The catalytic current is observed only for low concentrations of dioxygen.

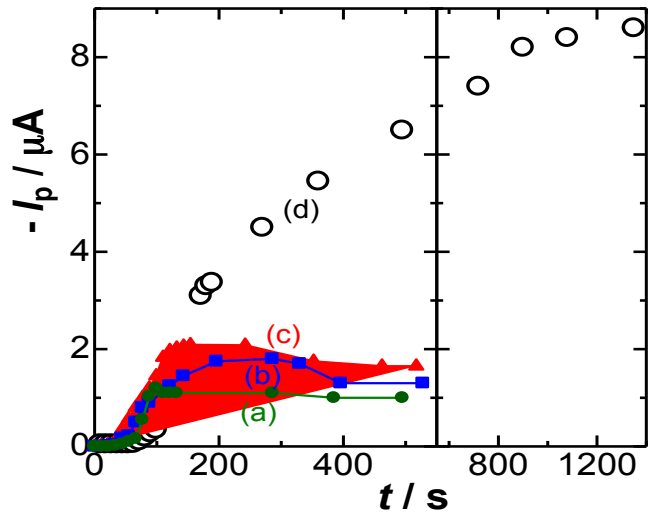


**Figure.8.** Time-variations of the peak currents for $v$ = 0.1 V $s^{-1}$ in (a) 0.09 mM, (b) 0.17 mM, (c) 0.33 mM, and (d) 0 mM hemin including 0.15 MTBA$ClO_4$ DMSO solutions after air was bubbled into the solutions, where the peak for (a)-(c) was at -0.7 and that for (d) was at -1.3 V.

These variations are consistent with those in Fig. 6 and 7.

### 3.3.2 Model of adsorbed hemin

The scan rate-dependence of the catalytic currents in Fig. 3(b) seems to resemble the general adsorption behavior in that the peak currents deviate upward from the line proportional to $v^{1/2}$ at fast scans. When the peak currents are plotted against $v$, they fall on a line in Fig. 9 (a), but show an intercept. Therefore the current does not belong to a surface wave. If the catalytic component is superimposed on the diffusion current, the total current should be expressed by $I_p = k_1 v^{1/2} + k_2 v$ for constants $k_1$ and $k_2$ [80]. The plot of $\Delta I_p = I_p - k_1 v^{1/2}$ against $v$ showed proportionality in Fig. 9(b). If the peak current

density of the surface wave is caused by the simple adsorption with the form of $(F^2/RT)\Gamma v$ [92], the amount of the adsorbed species, $\Gamma$, is calculated to be $5\times10^{-9}$ mol $cm^{-2}$ on the assumption of a one-electron transfer reaction. This value is close to the accepted values of the monolayer adsorption as well as reported values of adsorbed hemin [64,93,94]. The monolayer adsorption infers that the catalysis of $O_2$ should occur only by the absorbed amount without supply of $O_2$ by diffusion. Therefore, a possible mechanism of the catalytic current is:

$$\text{hem}(Fe^{2+})_{ad} + O_2 \rightarrow \text{hem}(Fe^{2+})_{ad}\text{-}O_2 \quad (5)$$

$$\text{hem}(Fe^{2+})_{ad}\text{-}O_2 + e^- \rightarrow \text{hem}(Fe^{2+})_{ad}\text{-}O_2^- \quad (6)$$

Reaction (5) represents the uptake of dioxygen in the adsorbed layer, while (6) includes the electron transfer reaction corresponding either to the wave at -0.7 V or -0.9 V. If $\text{hem}(Fe^{2+})_{ad}\text{-}O_2^-$ was decomposed into $\text{hem}(Fe^{2+})_{ad}$ and soluble $O_2^-$ or its stabilized species, dioxygen in solution would be catalyzed one after another through reaction (5) with the help of diffusional supply of dioxygen. Continuous catalysis requires the reproduction of $\text{hem}(Fe^{2+})_{ad}$.

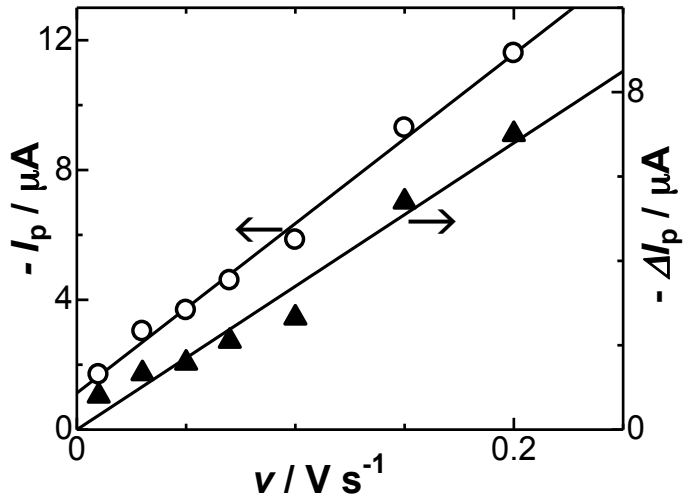


**Figure 9.** Scan rate dependence of the cathodic peak current at ca. -0.7 V in the (filled marks) deaerated and the (open marks) aerated 0.15 M $TBAClO_4$ + 0.40 mM hemin + DMSO solution at the (circles) GC, (squares) Au and (triangles) Pt electrodes

Adsorption depends generally on materials of substrates. Platinum and gold disk electrodes were used for the reduction of hemin instead of the glassy carbon. The reduction current densities of deaerated hemin solution at the Pt and the Au electrodes were almost the same as those at the GC electrode. They were also the same as in the aerated hemin solution. Consequently, the catalytic current can be observed only at the GC electrode. The formation of hem$(Fe^{2+})_{ad}$ seems to be restricted on carbon electrodes. The non-observation of catalytic current at the Pt and the Au electrodes is consistent with the slow reaction rate constant (5 min half-life) of the catalytic reaction estimated from the UV absorbance.

If hem$(Fe^{2+})_{ad}$-$O_2^-$ can be removed electrochemically from the electrode, potential control is expected to continue the catalytic reaction intermittently. When the potential was cycled in the domain from -0.8 to 0.0 V in aerated hemin solution, the catalytic current decreased with the number of the scans, as shown in Fig.10(c, d). The voltammograms cycled in the domain from -0.8 V to 0.6 V did not vary with the number of scans Fig.10(a, b). The invariance to the number of scans indicates that the anodic wave at 0.3 V should work as the removal of the adsorbed species. So far as potential is cycled between -0.8 V and 0.3 V, the dioxygen can be catalyzed intermittently. The catalytic reaction is, however, not under steady state.

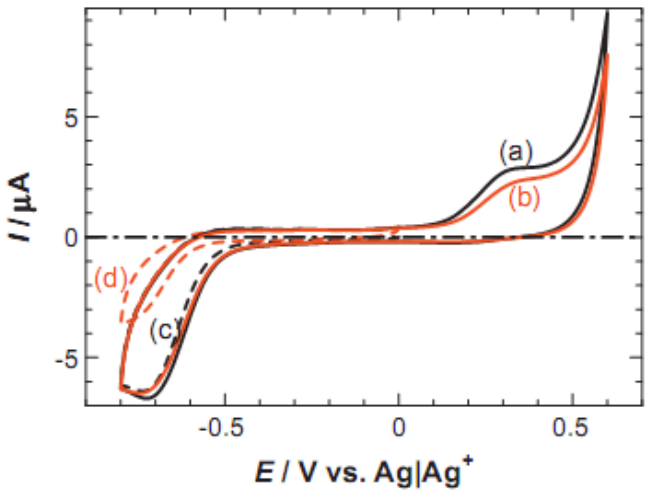

**Figure.10.** Voltammograms in aerated DMSO solution including 0.4 mM hemin+0.15 M TBAClO4 at the first(a,c) scan and the 20$^{th}$(b,d) scan in two scan domains(c,d: from -0.8 to 0.0 V) and (a,b: from -0.8 to 0.6 V) for v=0.1Vs$^{-1}$.

The Fig.11(c) indicated that the species which was oxidized were from the product which were produced at -0.65 V and -0.9 V by comparing the currents with Fig.11(d)( $Ipc/_{0.3}$=3.9 μA , $Ipd/_{0.3}$=2.5μA). The CV results implied that the peak which is at 0.3V dues to peaks which are at -0.65 V and -0.9 V.

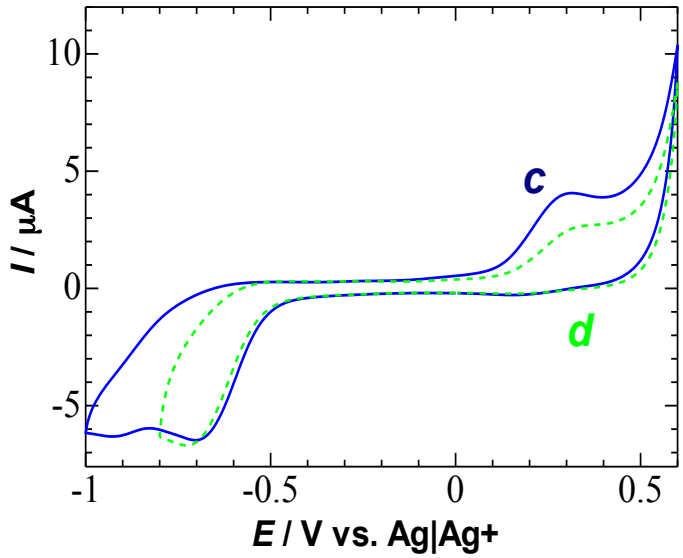


**Fig.11.** Voltammogrames in aerated 0.33 mM hemin in 0.15 M TBAP + DMSO at the glassy carbon electrode for v=0.1Vs$^{-1}$

The Fig.12 showed the voltammograms in aerated hemin solution. Fig.12(e) was obtained in beginning of the experiment, along with the time, the $HmFe^{3+}$ was reduced to $HmFe^{2+}$, without supplement as Fig.12(f) showed. Without oxidation reaction which happened at 0.3 V, may block the reaction cycle, which demonstrate that the anodic wave at 0.3 V should work as the removal of the adsorbed species. When dioxygen was bubbled into solution, we found the reduction peak current became larger which indicated chemical reaction $HmFe^{2+} + O_2 \rightarrow HmFe^{3+}$ happened as Fig.12(g) showed, but the reaction cycle was not continue because of adsorbed species.

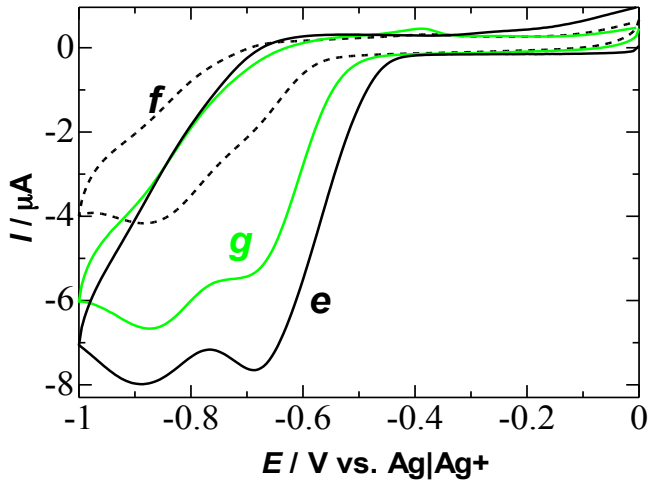


**Fig.12.** Voltammogrames in aerated 0.33 mM hemin in 0.15M TBAP + DMSO at the glassy carbon electrode for 0.1Vs$^{-1}$, e) first scan, f) tenth scan, g) eleventh scan (start bubbling oxygen into the solution)

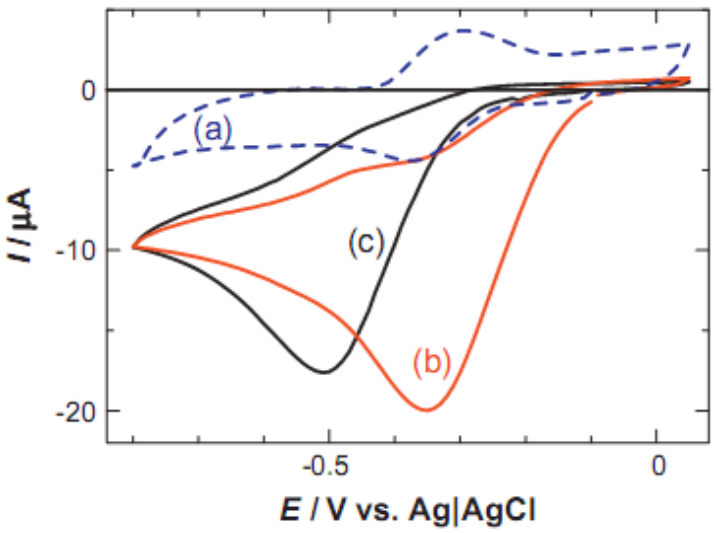


**Fig.13.** Voltammograms at the hemin-coated GC electrode in the deaerated(a) and aerated(b) 0.25 M KCl solution for the scanrate,0.1Vs$^{-1}$. Voltammogram(b) is in the aerated solution at the bare electrode.

Of interest is catalytic current of dioxygen by hemin in aqueous solution. Since hemin is not dissolved in aqueous solution, water was added to the DMSO solution

including 0.4 mM hemin so that water concentration was a few mM. The addition of water had no influence on the voltammograms. Therefore reactions (4) and (5) are valid in the presence of small amount of water.

It is interesting to examine the catalytic behavior in aqueous solution. Since hemin is not dissolved in aqueous solution. The GC electrode was coated with hemin-dissolved DMSO solution, and was dried at 60□ for 30 min. the thickness of the hemin film was 0.2 μm on the assumption of the film density, $1 g \cdot cm^{-2}$. Voltammetry at the hemin-coated electrode was made in the deaerated solution, as showed in Fig.10(a). the reduction at -0.36 V vs.Ag/AgCl was a surface wave, verified by the proportionality to the scan rates. The redox charge density was $7.5 \times 10^{-10} mol \cdot cm^{-2}$. Air-saturated solution showed only the cathodic wave(b), of which peak was located at the same potential as in the deaerated solution(a). Since the dioxygen at the bare electrode was reduced at -0.50V(c), the catalytic gain of the voltage is 0.14V, which is smaller than 0.50V in the DMSO solution. The catalytic peak current(b) was close to the sum of the peak current of(a) and the diffusion controlled peak current at the bare electrode(c). Unfortunately, it decreased with the time of the electrolysis(a few minutes), because the film was lost during the voltammetry.

### 3.4. Summary

Hemin can catalyze dioxygen in the form of an adsorbed adduct of hemin with dioxygen at glassy carbon electrodes. Since soluble hem($Fe^{2+}$) is not reproduced from the adsorbed adduct, the catalytic reaction does not belong to the Fenton reaction. The catalytic current cannot keep a steady state even if dioxygen is supplied to the electrode by diffusion or convention. Since the adsorbed species is dissolved at the oxidation at 0.3 V, the electrode surface is renewed sufficiently for the catalytic reaction. In order to continue the catalytic reaction, it is necessary to remove the adsorbed species.

Otherwise, the catalytic current is blocked gradually. Consequently, the catalysis of dioxygen by hemin is not suitable for an alternative to precious metals in fuel cells.

# Chapter 4

## Relationship between electrochemical catalysis and the carriage of dioxygen by hemin

### 4.1. Introduction

Hemin, iron(III) protoporphyrin IX, not only takes a central role in the redox activity of several heme-proteins [95-97] but also works as an oxygen-carrier for mammalian respiration [98 - 104] through myoglobin and hemoglobin. Furthermore, it exhibits electrocatalytic properties of detecting hydrogen peroxide [105 - 113], dioxygen [105,110,114-123], nitrogen oxides [97,106,112,124], superoxides [125], neurotransmitters [126,127] and tryptophan [128]. The redox activity in heme-proteins may be similar to the electrocatalysis from a viewpoint of the combination of chemical reactions with electron transfer steps. In contrast, the carriage of dioxygen is not associated explicitly with the catalysis.

The electrocatalysis of the reduction of dioxygen occurs in the following steps [109,112,114,120,123]: ferric hemin is reduced electrochemically at the potential at which dioxygen is not reduced; the generated ferrous hemin reduces dioxygen to be retrieved to the ferric form, which induces the reduction current. In contrast, it is ferrous hemin that transports dioxygen in mammalian respiration as an adduct of dioxygen rather than ferric hemin [98-103]. The stability of the adduct has been explained in terms of the steric effects [102,104,129,130]. The formation of the adduct does not lead directly to the catalytic mechanism, in that ferrous hemin encountering dioxygen is converted to the ferric type to lose the ability of the carriage. This question is not always true when hemin is dissolved to solution in which the catalysis has hardly been observed [131]. It inspires us to examine the catalytic mechanisms by paying attention to the catalytic conditions.

Here, we compare the catalytic effects of dioxygen at adsorbed hemin with those in dissolved hemin in order to solve the question.

## 4.2. Experimental

Hemin (Wako) with nominal 97 % purity was stored in a refrigerator. It was not weighed until it was left at a room temperature for a long time in order to avoid mixing with water. Dimethyl sulfoxide (DMSO) which was distilled under reduced pressure was dried with molecular sieves. Water was distilled and deionized.

All electrochemical experiments were performed in a three-electrode cell including a Pt wire auxiliary electrode, a reference electrode and the glassy carbon (GC) working electrode 3 mm in diameter. The reference electrode was a $Ag/Ag^{+}$(0.01 M ( = mol $dm^{-3}$) $AgNO_3$) for DMSO solution or a Ag|AgCl (3.5 M KCl) electrode for aqueous solution. When hemin-included DMSO solution was dropped on the GC electrode, it dispersed uniformly not only to the GC electrode but also to the insulating wall made of polyetherketone 6 mm in diameter. The actual amount of hemin on the electrode was multiplied by $(3/6)^2$. A potentiostat used was Compactstat (Ivium, Netherlands).

Spectro-electrochemical measurements was made with V-570 UV/VIS/NIR Spectrophotometer (Jasco, Japan) by use of a thin layer cell made of quartz 0.47 mm thick, into which the Pt mesh 0.076×50×10 $mm^3$ with the density 80 lines per inch was inserted [131].

## 4.3. Results and Discussion

### 4.3.1 Catalytic current of dioxygen by hemin films

Figure 1(a) shows voltammograms in deaerated phosphate buffer solution 0.20 M, pH

7.4 (25 °C)at the GC electrode coated with the hemin film, where 30 μm$^3$ DMSO solution including 0.010 mM hemin, i.e. 0.30 nmol hemin was dispersed on the electrode and was dried at 60 °C. The reduction and the oxidation peaks appeared at -0.37 V and -0.22 V vs. Ag|AgCl, respectively. Since the cathodic peak currents were proportional to the scan rate, $v$, for $0.05 < v < 1.0$ V s$^{-1}$, the current should be controlled by the surface reaction of the adsorbed ferric hemin. When air was bubbled in the solution, the reduction peak current was enhanced, as shown in Fig. 1(b). Then the oxidation peak disappeared, indicating that hem($Fe^{2+}$) should be consumed by fast chemical complications. In contrast, dioxygen was reduced at the bare GC electrode at the potential 0.45 V more negative than the reduction of hemin (Fig. 1(c)). Consequently the enhanced current at -0.30 V vs. Ag|AgCl by the air bubbling can be regarded as the catalytic current of dioxygen by hemin. When dioxygen gas under 1 atm was bubbled in the solution, the peak current at the hemin-coated electrode increased 5 times larger than the current by air. This result supports the electrocatalysis of dioxygen.

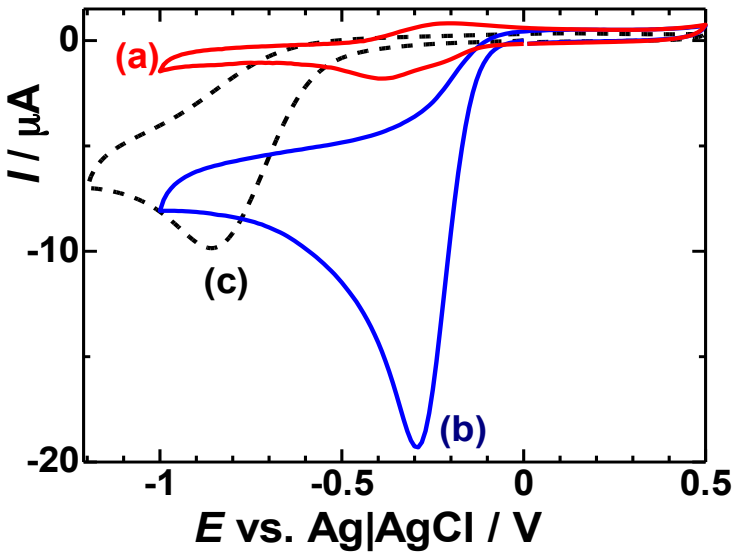


Fig. 1 Voltammograms at the hemin-coated GC electrode in (a) deaerated and (b) aerated phosphate buffer solution 0.20 M, pH 7.4 (25℃) for $v$ = 0.1 V s$^{-1}$, where a drop of 30 μm$^3$ with 0.010 mM (M = mol dm$^{-3}$) hemin, corresponding to 0.30 nmol hemin, was cast on the electrode. Voltammogram (c) is at the bare GC electrode in the aerated solution

The electric charge density was evaluated from i) drawing a background line along the cathodic wave of Fig. 1(a) at -0.7 V and 0.1 V, ii) integrating the domain encircled with the wave and the background line, iii) dividing the area by the scan rate, and iv) dividing the resulting charge by the geometrical area of the electrode. It was $1.1\times10^{-9}$ mol $cm^{-2}$. It corresponds to the area $(0.4\ nm)^2$ per adsorbed hemin molecule if hemin are adsorbed uniformly on the electrode. If surface roughness (ranging from 2 to 5 supposedly as used conventionally for electrode surfaces) is taken into account, the area per adsorbed hemin molecule is close to the projected area of the molecule. According to the model of catalysis caused by adsorbed species [132], the reaction rate is assumed to have a linear relation with the surface concentration, $\Gamma$, of the adsorbed species. In order to examine this assumption, we obtained variations of the catalytic peak currents at -0.3 V vs. Ag|AgCl with surface concentrations of hemin, as shown in Fig. 2.

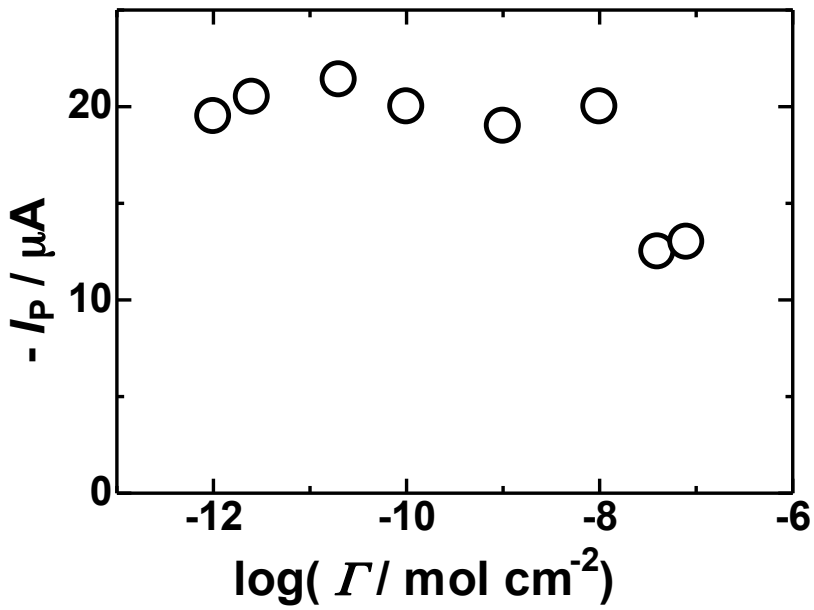


Fig. 2. Dependence of the catalytic peak currents on the molar density of adsorbed hemin, observed in aerated phosphate buffer solution, 0.20 M pH 7.4 (25℃) at the GC electrode.

The peak current did not vary with $\Gamma$ for $\Gamma < 10^{-9}$ mol $cm^{-2}$. Therefore the adsorbed concentration of ferric hemin is large enough for the consumption of dioxygen. Even

the thinnest film, $\Gamma$ = 1.1×10$^{-12}$ mol cm$^{-2}$ corresponding to the area (12 nm)$^2$ per adsorbed hemin molecule, did not suppress the catalytic current. If this surface concentration were to be layered with each 12 nm separation, the volume concentration of hemin would become 0.9 mM. This concentration is still larger than the concentration of dioxygen saturated by air, 0.5 mM. As a result, the catalytic current is not controlled by surface concentrations of hemin for 10$^{-12}$ < $\Gamma$ < 10$^{-9}$ mol cm$^{-2}$, but is controlled by the concentration of dioxygen through the catalytic reduction. On the other hands, the catalytic current decreased with an increase in the surface concentration for $\Gamma$ > 7.4×10$^{-9}$ mol cm$^{-2}$. The thick films obviously block the transport of the charge in the film, and hence suppress the current.

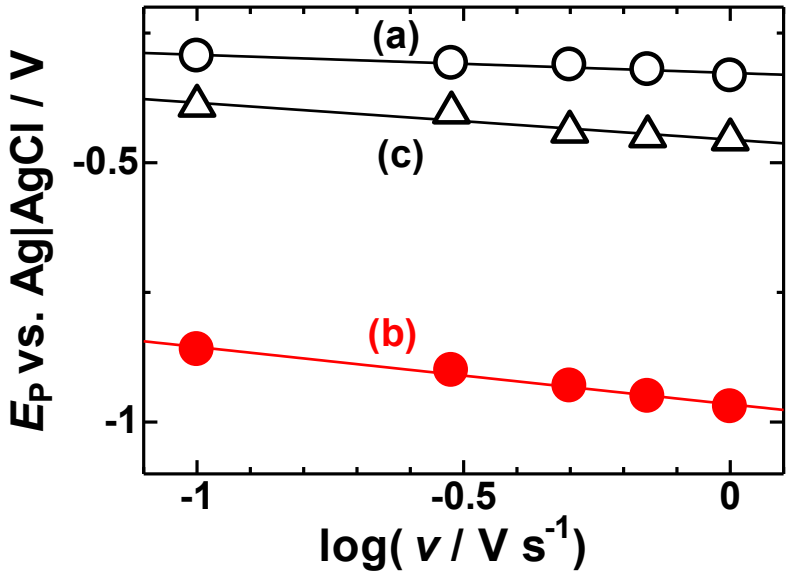


Fig. 3. Variations of the cathodic peak potentials with the logarithmic scan rates at the hemin-coated electrode ($\Gamma$ = 1.1×10$^{-9}$ mol cm$^{-2}$) in the (a) aerated and (c) deaerated phosphate buffer solution 0.2 M, pH 7.4 (25℃). The peak potentials (b) were obtained at the bare GC electrode in the aerated solution.

Figure 3 shows dependence of (a) the catalytic peak potentials, $E_p$, and (b) the reduction peak potentials at the bare GC electrode on the logarithmic scan rates. The comparison between the two indicates that the catalytic reaction decreases the

overpotential by 0.5-0.6 V. Both plots fall each line, the slope of which are 0.04 V and 0.14 V for the catalysis and the direct reduction, respectively. The peak potentials of the catalytic currents are close to those of the reduction peak of adsorbed hemin without dioxygen (c), where the determination of the latter contained errors ca. 0.03 V. The similarity indicates that the catalytic potential shift (a) by the scan rate should be caused by the potential shift of adsorbed hemin (c). In other words, the catalytic current itself does not provide any potential shift by the scan rates.

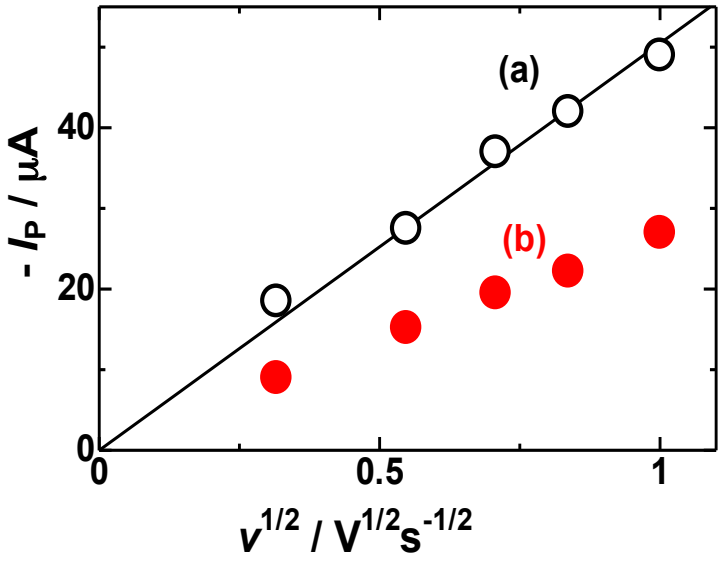


Fig. 4. Dependence of the cathodic peak currents of dioxygen at (a) the hemin-coated GC electrode and (b) the bare GC electrode on the square-roots of the scan rates, where dioxygen was supplied from air.

Figure 4(a) shows variations of the catalytic peak current with the square-roots of the scan rate. Since the currents were proportional to $v^{1/2}$, they ought to be controlled by diffusion of dioxygen. In contrast, the reduction peak currents at the GC bare electrode (b) were not only unproportional to $v^{1/2}$, but also were smaller than half the catalytic currents (a). They may be associated with chemical complications rather than diffusion [133]. Some complications are supported by the large variation of $E_p$ vs log $v$ in Fig. 3(b). The slope of the proportional line in Fig. 4(a), 49 μA $V^{-1/2}$ $s^{1/2}$, is close to the slope value, 42 μA $V^{-1/2}$ $s^{1/2}$, calculated from the equation for the diffusion controlled current

at the successive two-electron transfer reaction ($n = 2$) [134],

$$I_p = -0.446nFAc^*(DvF/RT)^{1/2} \quad (1)$$

where the concentration of dioxygen by air saturation $c^*$ was 0.5 mM at 25 °C, the diffusion coefficient of dioxygen $D$ was $1.96\times10^{-5}$ cm$^2$ s$^{-1}$ [135], and $A$ is the electrode area. Eq. (1) is different from the well-documented expression by $n^{3/2}$. The approximate agreement between the experimental value of $I_p$ and Eq. (1) indicates that dioxygen can be quantitatively determined by hemin-coated electrodes only when $\Gamma < 10^{-9}$ mol cm$^{-2}$.

The electron transfer number, two, suggests the following reaction mechanisms:

$$O_2 + 2\text{hem}(Fe^{2+}) \rightarrow O_2^{2-} + 2\text{hem}(Fe^{3+}) \quad (2)$$

$$2\text{hem}(Fe^{3+}) + 2e^- \rightarrow 2\text{hem}(Fe^{2+}) \quad (3)$$

The reported values of $n$ for the catalytic reduction of dioxygen by hemin are one [112], two [109] and four [114,120].

## 4.3.2 Reaction of dissolved hemin with dioxygen

The hemin-dissolved DMSO solution showed only the diffusion-controlled current of hemin at the platinum or the gold electrode without any catalytic reaction [131]. In contrast, the GC electrode at which hemin was naturally adsorbed exhibited a small contribution of the catalytic currents for the reduction of dioxygen [131]. The catalysis seems to require (A) water in solution and (B) adsorbed hemin rather than dissolve hemin. In order to examine (A), we made voltammetry in the aerated DMSO solution to which water was added gradually. The reduction peak currents were proportional to $v^{1/2}$, independent of addition of water. This fact proves that water does not cause the catalysis. Condition (B) implies a property of an adsorbed state different from a dissolved state. A possible property as to the difference is concentration. We increased concentrations of dissolved hemin in DMSO to see whether the reduction current included a catalytic component or not. Figure 5 shows the variation of the reduction

peak current at the platinum electrode in the aerated DMSO solution. The currents for concentrations less than 0.5 mM were proportional to the concentrations on hemin and $v^{1/2}$, indicating the diffusion control [131]. Those for concentrations over 0.7 mM had a quadratic relation with the concentration, as shown in the dashed curve in Fig. 5. The component over the proportional line should be due to the catalysis.

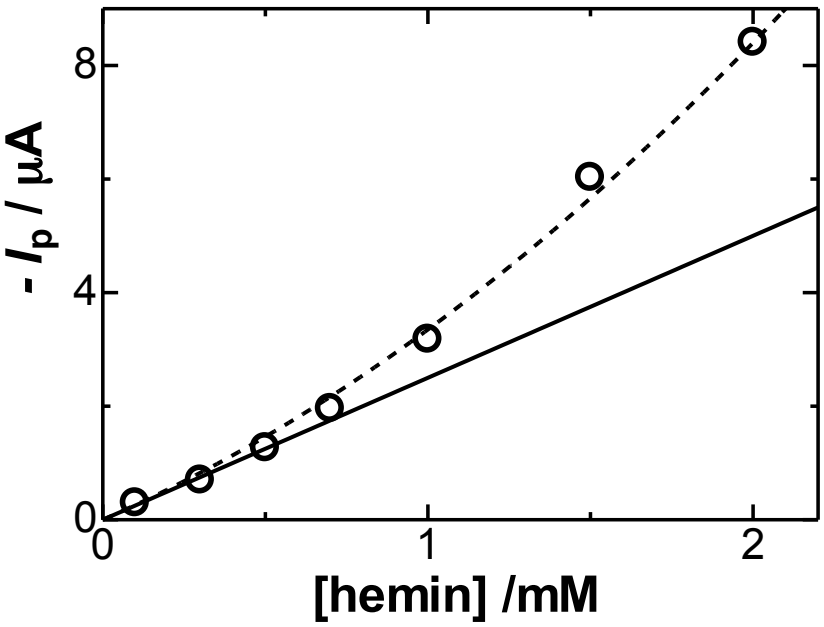


**Fig.5.** Variation of the cathodic peak currents with the concentrations of hemin in the aerated DMSO solution at $v$ = 0.1 $Vs^{-1}$. The dotted curve is fitted to $-I_p = 2.5$ [hemin] + 0.85 [hemin]$^2$.

We consider tentatively the dioxygen adduct of hemin:

$$O_2 + 2\text{hem}(Fe^{2+}) \leftrightarrow (\text{hem}(Fe^{2+}))_2O_2 \quad (4)$$

The stability constant for $(\text{hem}(Fe^{2+}))_2O_2$ is expressed by

$$K = [(\text{hem}(Fe^{2+}))_2O_2]/[O_2][\text{hem}(Fe^{2+})]^2 \quad (5)$$

If the adduct is decomposed through

$$(\text{hem}(Fe^{2+}))_2O_2 \rightarrow O_2^{2-} + 2\text{hem}(Fe^{3+}) \quad (6)$$

the catalytic current is observed, which is controlled by the decomposition rate of the

adduct, i.e. $k_d$[(hem($Fe^{2+}$))$_2O_2$], where $k_d$ is the decomposition rate constant. Since the observed current in the aerated solution of dissolved hemin is the sum of the catalytic current and the diffusion controlled current, the substitution of [hem($Fe^{2+}$)] for [(hem($Fe^{2+}$))$_2O_2$] by use of Eq. (5) yields

$$-I_p = 0.446FA[\text{hem}(Fe^{2+})](DvF/RT)^{1/2} + k_dK[O_2][\text{hem}(Fe^{2+})]^2 \quad (7)$$

Then the current is expressed by a quadratic equation of hemin concentration, as can be demonstrated by Fig. 5. Concentrations of dissolved species for voltammetry are usually less than 1 mM, whereas those for adsorbed species are more than a few molarities. Therefore the second term in Eq. (7) for the adsorbed hemin is larger by $10^6$-$10^8$ larger than that for the dissolved hemin. This estimation explains the appearance of the catalysis at the hemin-coated electrode.

We try to find formation of the dioxygen adduct in reaction (4) spectroscopically under our experimental conditions without any enzymatic support. Ferrous hemin was generated electrochemically at the platinum mesh electrode in a thin layer cell through which a monochromatic beam was passed. Figure 6 shows UV-vis spectra for (a) ferric hemin and (b) electrochemically reduced hemin. Ferric and ferrous hemins show the Soret band at 404 nm and 424 nm, respectively, being close to bibliographic values [104,129,136-139]. As hemin($Fe^{3+}$) was reduced electrochemically, the absorbance at 424 nm increased at the expense of the absorbance at 404 nm. When dioxygen was added to the hemin($Fe^{2+}$) solution after the cathodic electrolysis, the absorbance at 404 was partially restored, implying the oxidation of the ferrous ion by dioxygen into ferric ion. However, the band at 404 nm is overlapped with the species generated when dioxygen is added to hem($Fe^{2+}$) [136,138]. Since the band at 424 nm is specific to hem($Fe^{2+}$), it is obvious that purging dioxygen to the hem($Fe^{2+}$) solution decreased the concentration of hem($Fe^{2+}$) by a half (c). The enhancement of the absorbance at 404 nm can be attributed either to the hem($Fe^{3+}$) or the dioxygen adduct. The inset of Fig. 6 shows the bands at 621 nm for hem($Fe^{3+}$), which is specific to hem($Fe^{3+}$) discriminating against hem($Fe^{2+}$) [138,140]. The

addition of dioxygen to hem($Fe^{2+}$) did not exhibit the band at 621 nm, retrieving the band at 404 nm. This result indicates that hem($Fe^{2+}$) should not be oxidized simply to hem($Fe^{3+}$) but be converted to other species, e.g. the dioxygen adduct, which is detected at 404 nm. This is a confirmation of reaction (4).

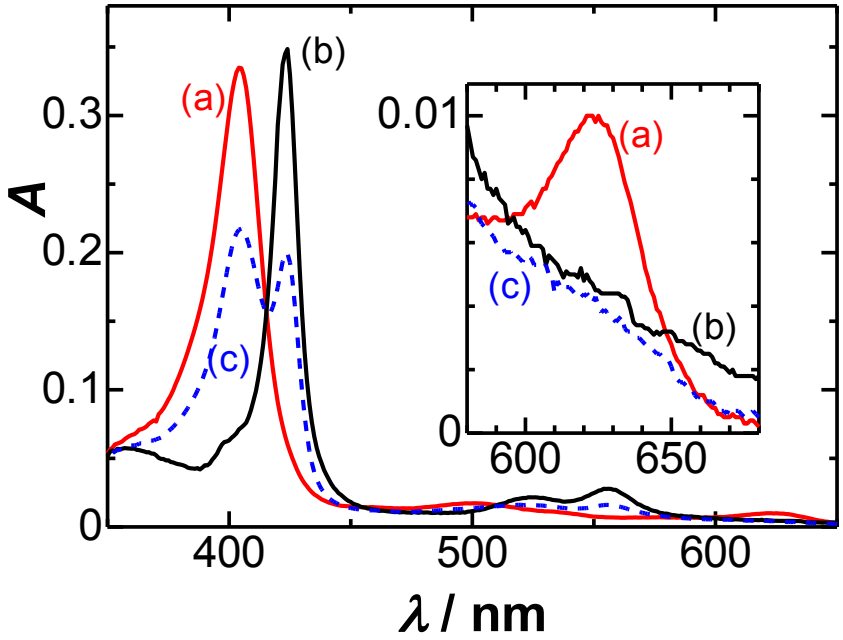


Fig. 6. UV-vis spectra of (a) hem($Fe^{3+}$), (b) hem($Fe^{2+}$) and (c) dioxygen-added hem($Fe^{2+}$) for 30 s in the UV-electrochemical, thin layer cell including 0.032 mM hemin + DMSO. The thickness of the cell was 0.4 mm into which the platinum mesh-electrode (150 mesh) was inserted. The reduction was made at -0.6 V vs. Ag|AgCl.

When the reduction potential of hemin is applied to the electrode, hem($Fe^{3+}$) near the electrode is consumed by the electrode reaction. Then the forward rate in Eq. (7) increases to depress [(hem($Fe^{2+}$))$_2O_2$]. As a result, the adduct has not been recognized in electrochemically catalytic experiments.

### 4.4. Summary

The catalytic current of dioxygen at the hemin-coated electrode is controlled by diffusion of dioxygen at the reduced potential of hem($Fe^{3+}$) with successive

two-electron reduction, independent of surface concentrations of hemin for $\Gamma < 10^{-9}$ mol $cm^{-2}$. The diffusion-controlled step without essential potential shift indicates that no reaction rate constant in Eq. (2) can be evaluated from the present voltammetric data. The catalytic current is not observed at the bare electrode in hemin-dissolved solution for [hem($Fe^{3+}$)] < 0.5 mM, but it can be for [hem($Fe^{3+}$)] > 1 mM. The catalytic current is proportional to the quadratic relation of hemin concentrations. The quadratic relation can be ascribed to the stoichiometry of the reaction of two ferric hemin molecules with one dioxygen molecule to generate the dioxygen adduct.

The dioxygen adduct can be regarded as an intermediate of the catalytic reaction, given by reaction (4). It is decomposed to generate hem($Fe^{3+}$) by Eq. (6), which is reduced electrochemically to yield the catalytic current. As the electrochemical reduction proceeds, [hem($Fe^{3+}$)] decreases electrochemically at the expense of the adduct. Therefore the adduct is not directly detected by voltammetric measurements.

# Chapter 5

## Conclusion

Hemin in aerated dimethylsulfoxide catalyzes reduction of dioxygen at glassy carbon electrodes in the adsorbed state. A gain voltage for the catalysis is 0.5 V. The catalytic rate, being observed as the reduction current, increases with an increase in concentrations of dioxygen, but reaches a maximum at 6% of the saturated concentration. The chronoamperometric current for the catalysis decays to zero. These variations are different from the ordinary catalytic mechanism, in which hemin oxidized by dioxygen might be reused as the electrochemical reduction. The voltammetric peak current in deaerated hemin solution is diffusion controlled, whereas that in aerated solution is represented as a sum of the diffusion current and a surface wave. The catalytic current is caused by hemin incorporated with dioxygen, of which adsorption density is close to an amount of a monolayer. Therefore hemin films are not suitable for continuous reduction of dioxygen. Once the adsorbed layer is oxidized to remove the adsorption film, the catalytic reduction wave is retrieved.

The catalytic current at the hemin-coated electrode is confirmed to occur at the stoichiometry of two hemin molecules and one dioxygen molecule：

$$O_2 + 2\text{hem}(Fe^{2+}) \rightarrow O_2^{2-} + 2\text{hem}(Fe^{3+})$$

$$2\text{hem}(Fe^{3+}) + 2e^- \rightarrow 2\text{hem}(Fe^{2+})$$

Dioxygen can be catalyzed by hemin of which concentration is higher than concentration of dioxygen. Since the adsorbed film takes extremely high concentrations of hemin, the catalytic current is not controlled by the amount of adsorbed hemin but is determined by concentration of dioxygen. Therefore the catalytic current is controlled by diffusion of dioxygen, associated with the successive two-electron transfer reaction. The hemin-coated electrode can be used quantitative determination of dioxygen without

rigorous control of the amount of hemin.

The dioxygen adduct can be regarded as an intermediate of the catalytic reaction, given by reaction：

$$O_2 + 2\text{hem}(Fe^{2+}) \leftrightarrow (\text{hem}(Fe^{2+}))_2O_2 \rightarrow O_2^{2-} + 2\text{hem}(Fe^{3+})$$

It is not detected in voltammetry because the reduction potential of hemin decreases concentrations of not only ferric hemin but also the adduct through reaction (4). The stoichiometry, two, of hemin molecules causes a quadratic relation of the peak current with the concentration of dissolved hemin.

# References

[1] Respiratory Function of Hemoglobin. Connie C.W. Hsia, M.D. N Engl J Med 1998, 338:239-248 January 22, 1998

[2] H.Nishide,H.ohno and E.Tsuchida,Makromol. Chem.Rapid Commun.2(1981)55

[3] G-X,Wan, K.Shigehara,E.Tsuchida and E.C.Ason. J.Am.Chem.Soc.105(1983)2710

[4] N.Uotani.E.Hasegawa,H.Nishide and E.Tsuchida, J.Inorg.Biochem..22(1984)85.

[5] E.Tsuchida,H.Nishide,Y.Sato, J.Chem.Soc.,Chem Commun.,10(1982)556

[6] L.A.Bottomley and K.M.Kadish.Inorg.Chem.,20(1981)1348

[7] L.A.Constant and D.G.Davis, J.Electroanal,Chem.,74(1976)85

[8] D.G.Davis and R.F.Martin, J.Am.Chem.Soc.,88(1966)1365

[9] C.A.Marrese,E.A.Blubaugh and R.A.Durst, J.Electronanl,Chem..243(1988)193

[10] Ji Chen, Lu Zhao,Gaoquan,Shi. Journal of ELECTROANALYTICAL Chemistry 657(2011)34-38)

[11] Rongzhong, Jiang, Dat T.Tran, Deryn Chu. Electrochimica Acta 75(2012)185-190

[12] Jian Chen, Ulla Wollenberger, W.Scheller. Sensors and Actuators B 70(2000)115-120

[13] Y. Gao, J. Chen, J. Electroanal. Chem. 578 (2005) 129

[14] F. Arifuku, K. Iwatani, K. Ujimoto and H. Kurihara, Bull. Chem.Soc. Jpn. 60 (1987) 1661

[15] C. Shi and F.C. Anson, Inorg. Chem. 31 (1992) 5078

[16] A. Holmes-Smith, A. Hamill, M. Campbell and M. Uttamlal, Analyst 124 (1999) 1463

[17] A.M. Toader, V.Lazarescu. Electrochimica Acta 56(2010)863-866

[18] D.A.Foucher, C.H. Honeyman, J.M.Nelson, B.Z.Tang, I.Manners, Angew.Chem.Int.Ed.Engl.32(1993)1709

[19] K.S.Suslick, S.van, Duesen-Jeffries, in: K.S. Suslick (Ed). Comprehensive Supramolecular Chemistry, vol.5, Elsevier, Oxford,1996, pp.141-170

[20] T. Sagara, S. Takeuchi, K. Kumazaki, N. Nakashima, J. Electroanal. Chem. 396(1995) 525]

[21] Z. Brusova, E. Magner, Biolectrochemistry 76 (2009) 63

[22] N. Kamiya, S. Furusaki, M. Goto, Biotechnol. Lett. 19 (1997) 1015

[23] J. Lancaster, Nitric Oxide: Principles and Actions, Academic Press, San Diego,1996

[24] Y. Gao, J. Chen, J. Electroanal. Chem. 578 (2005) 129

[25] D.G. Wu, D. Cahen, P. Graf, R. Naaman, A. Nitzan, D. Shvarts, Chem. Eur. J. 7(2001) 1743

[26] M.A. Garcia, M. Losurdo, S.D. Wolter, T.H. Kim, W.V. Lampert, J. Bonaventura,G. Bruno, M. Giangregorio, A. Brown, J. Vac. Sci. Technol. B 25 (2007) 1504

[27] O. Elmouahid, C. Coutanceau, E.M. Belgsir, P. Crouigneau, J.M. Leger and C. Lamy, J. Electroanal. Chem. 426 (1997) 117

[28] E. Tsuchida, K. Yamamoto and K. Oyaizu, J. Electroanal Chem.438 (1997) 167

[29] AL. Bouwkamp-wijinoltz, W. Visscher and J.A.R. van Veen, Electrochim. Acta 43 (1998) 3141

[30] F. Arifuku, K. Iwatani, K. Ujimoto and H. Kurihara, Bull. Chem.Soc. Jpn. 60 (1987) 1661

[31] A. Holmes-Smith, A. Hamill, M. Campbell and M. Uttamlal, Analyst 124 (1999) 1463

[32] R.ZH. Jiang and SH.J. Dong, J. Phys. Chem. 94 (1990) 7471

[33] C. Shi and F.C. Anson, Inorg. Chem. 31 (1992) 5078

[34] F. Arifuku, K. Mori, T. Muratani and H. Kurihara, Bull. Chem.Soc. Jpn. 65 (1992)

1491

[35] V. Rajendran, E. Csoregi, Y. Okamoto and L. Gorton, Anal.Chim. Acta. 373 (1998) 241

[36] K. Yamamoto, T. Ohgaru, M. Torimura, H. Kinoshita, K. Kano and T. Ikeda, Anal. Chim. Acta. 406 (2000) 201

[37] F. Bedioui, J. Devynck and C. Bied-Charr34eton, J. Mol. Catal. A.113 (1996) 3

[38] T. Lotzbeyeer, W. Schuhmann and H.L. Schmidt, J. ElectroanalChem. 395 (1995) 341

[39] R.ZH. Jiang and SH.J. Dong, Electrochim. Acta 35 (1990) 1227

[40] R.R.Durand,F.C.Anson,JournaloftheElectrochemicalSociety129(1982)C116

[41] R.Z.Jiang,S.Dong,JournalofElectroanalyticalChemistry246(1988)101

[42] R.Z.Jiang,S.Dong,JournalofPhysicalChemistry94(1990)7471

[43]O.Ikeda,H.Fukuda,H.Tamura,JournaloftheChemicalSociety,FaradayTrans-actions82 (1986)1561

[44] S.Dong,R.Z.Jiang,BerichtederBunsen-Gesellschaft–PhysicalChemistry ChemicalPhysics91(1987)479

[45] R.Z.Jiang,D.Chu,JournaloftheElectrochemicalSociety147(2000)4605

[46]A.V.Palenzuela,L.Zhang,L.Wang,P.L.Cabot,E.Brillas,K.Tsay,J.J.Zhang,Electrochi micaActa56(2011)4744

[47]K.C.Lee,L.Zhang,H.S.Lui,R.Hui,Z.Shi,J.J.Zhang,ElectrochimicaActa54(2009)4704

[48] G.Wu,K.L.More,C.M.Johnston,P.Zelenay,Science332(2011)443

[49] Z.X.Liang,H.Y.Song,S.J.Liao,JournalofPhysicalChemistryC115(2011)2604

[50] Z.X.Liang,H.Y.Song,S.J.Liao,JournalofPhysicalChemistryC115(2011)2604

[51] Robert S.Tieman, Louis A.Coury Jr.*, William R.Heineman J.Electroanal.Chem, 281(1990)133-145

[52] M.Sosna, J-M. Chretien, J.D.Kilburn, P.N.Barlett, Phys.Chem. Chem.Phys.

12(2010) 10018-10026

[53] R. Jasinski, Nature 201 (1964) 1212-1213.

[54] M. Brezina, Ber. Bunsen Gesel. 77 (1973) 849-852.

[55] M. Brezina, A. H.-Matejkova, Collect. Czech. Chem.Commun. 38 (1973) 3024-3031.

[56] N. Zheng, Y. Zeng, P.G. Osborne, Y. Li, W. Chang, Z. Wang, J. Appl. Electrochem. 32 (2002) 129-133.

[57] S. Antoniadou, A.D. Jannakoudakis, E.Theodoridou, Synth.Met.30 (1989) 283-294.

[58] F. Arifuku, K. Mori, T. Muratani, H. Kurihara, Bull. Chem. Soc. Jpn. 65(1992) 1491-1495.

[59] Z.X. Liang, H.Y.Song,S.J. Liao, J. Phys. Chem.C, 115 (2011) 2604-2610.

[60] N. Kobayashi, T. Osa, J. Electroanal. Chem. 157 (1983) 269-281.

[61] Q. Ma, T. Liu, T. Tang, H. Yin, S. Aia, Electrochim. Acta 56 (2011) 8278-8284.

[62] J. Chen, L. Zhao, H. Bai, G. Shi, J. Electroanal. Chem. 657 (2011) 34-38.

[63] J.-S. Ye, Y. Wen, W.D. Zhang, H.-F. Cui, L.M. Gan, G.Q. Xu, F.-S. Sheu, J. Electroanal. Chem. 562 (2004) 241-246.

[64] F. Valentini, L. Cristofanelli, M. Carbone, G. Palleschi, Electrochim. Acta 63 (2012) 37-46.

[65] G.L. Turdean, I. C. Popescu, A. Curulli, G. Palleschi, Electrochim. Acta 51 (2006) 6435-6441.

[66] Y. Gao, J. Chen, J. Electroanal. Chem. 578 (2005) 129-136.

[67] J.B. Xu, T.S. Zhao, L. Zeng, Int.J, Hydrogen Energy, 37 (2012) 15976-15982.

[68] M. Lefevre, E. Proietti, F. Jaouen, J.P. Dodelet, Science 324 (2009) 71-74.

[69] R. Jiang, D.T. Tran, J.P. McClure, D. Chu, Electrochim. Acta 75 (2012) 185-190.

[70] C. Guo, C. Chen, Z. Luo, Int. J. Electrochem. Sci. 8 (2013) 8940-8950.

[71] P.-B. Xi, Z.-X. Liang, S.-J. Liao, Int. J. Hydrogen Energy, 37 (2012) 4606-4611.

[72] Q. Yang, Y. Nie, X. Zhu, X. Liu, G. Li, Electrochim. Acta 55 (2009) 276-280.

[73] M.T. de Groot, M. Merkx, A.H. Wonders, M.T.M. Koper, J. Am. Chem. Soc. 127 (2005) 7579-7586.

[74] C.-Z. Li, S. Alwarappan, W. Zhang, N. Scafa, X. Zhang, Am. J. Biomed. Sci. 1 (2009) 274-282.

[75] Y. Lai, Y. Ma, L. Sun, J. Jia, J. Weng, N. Hu, W. Yang, Q. Zhang, Electrochim. Acta 56 (2011) 3153-3158.

[76] Y.-L. Zhang, H.-X. Shen, J.-L. Sun, C.-X. Zhang, Electrochim. Acta 46 (2001) 2923-2928.

[77] G.S. Rao, Chem.-Bio. Interact. 80 (1991) 339-347.

[78] F. Haber, J. Weiss, Proc. R. Soc. London, A. 147 (1934) 332-351.

[79] R.S. Nicholson, I. Shain, Anal. Chem. 36 (1964) 706-723.

[80] K. Aoki, K. Tokuda, H. Matsuda, J. Electroanal. Chem. 199 (1986) 69-79.

[81] R.S. Tieman, L.A. Coury Jr., J.R. Kirchhoff, W.R. Heineman, J. Electroanal. Chem. 281 (1991) 133-145.

[82] G. Meyer, M. Savy, Electrochim. Acta 22 (1977) 213-215.

[83] M. Brezina, W. Khalil, J. Koryta, M. Musilova, J. Electroanal. Chem. 77 (1977) 237-244.

[84] H. Zhang, K. Aoki, J. Chen, T. Nishiumi, H. Toda, E. Torita, Electroanalysis, 23 (2011) 947-952.

[85] H. Cao, X. Sun, Y. Zhang, C. Hu, N. Jia, Anal. Methods, 4 (2012) 2412-2416.

[86] I. Inamura, M. Isshiki, T. Araki, Bull. Chem. Soc. Jpn. 62 (1989) 2413-2415.

[87] Y. K.-Konishi, H. Kihara, H. Suzuki, Eur. J. Biochem. 170 (1988) 589-595.

[88] J. Jin, L.S. Li, X. Wang, Y. Li, Y.J. Zhang, X. Chen, Y. Li, T. J. Li, Langmuir 15 (1999) 6969-6974.

[89] A. D. Ryabov, V. N. Goral, L. Gorton, E. Csöregi, Chem. Eur. J. 5 (1999) 961-967.

[90] A.J. Bard, L.R. Faulkner, Electrochemical Methods: Fundamentals and Applications, John Wiley & Sons, 2001, pp.505-505.

[91] K. Aoki, M. Ishida, K. Tokuda, J. Electroanal. Chem. 245 (1988) 39-50.

[92] A.J. Bard, L.R. Faulkner, Electrochemical Methods: Fundamentals and Applications, John Wiley & Sons, 2001, pp. 590-591.

[93] A.M. Toader, E. Volanschi, M.F. Lazarescu, V. Lazarescu, Electrochim. Acta 56 (2010) 863-866.

[94] T. Sagara, S. Takeuchi, K. Kumazaki, N. Nakashima, J. Electroanal. Chem. 396 (1995) 525-533.

[95] J. Xiea, X. Fenga, J. Hua, X. Chena, A. Li, Biosens. Bioelectr. 25 (2010) 1186–1192.

[96] N. Jia, Y. Wen, G. Yang, Q. Lian, C. Xu, H. Shen, Electrochem. Comm. 10 (2008) 774-777.

[97] K. Liu, J. Zhang, G. Yang, C. Wang, J.-J. Zhu, Electrochem. Comm. 12 (2010) 402-405.

[98] K. Imai, J. Mol. Biol. 133 (1979) 233-247.

[99] M. Brunori, R.W. Noble, E. Antonini, J. Wyman, J. Biol. Chem. 241 (1966) 5238-5243.

[100] M.H. Keyes, M. Falley, R. Lumry, J. Amer. Chem. Soc. 93 (1971) 2035-2040.

[101] J.P. Collman, J.I. Brauman, K.S. Suslick, J. Am. Chem. Soc. 97 (1975) 7185-7186.

[102] J.P. Collman, J.I. Brauman, K.M. Doxsee, T.R. Halbert, K.S. Suslick, Proc. Nati. Acad. Sci. 75 (1978) 564-568.

[103] C.-Z. Li, G. Liu, S. Prabhulkar, Am. J. Bio. Sci. 1 (2009) 303-311.

[104] T.G. Traylor, Acc. Chem. Res. 14 (1981)102-109.

[105] L. Shen, N. Hu, Biochim. Biophys. Acta 1608 (2004) 23-33.

[106] F. Valentini, L. Cristofanelli, M. Carbone, G. Palleschi, Electrochim. Acta 63 (2012) 37-46.

[107] G. L. Turdean, I. C. Popescu, A. Curulli, G. Palleschi, Electrochim. Acta 51 (2006) 6435-6441.

[108] Q. Yanga, Y. Niea, X. Zhub, X. Liua, G. Li, Electrochim. Acta 55 (2009) 276-280.

[109] Y. Gao, J. Chen, J. Electroanal. Chem. 578 (2005) 129-136.

[110] J. Chen, L. Zhao, H. Bai, G. Shi, J. Electroanal. Chem. 657 (2011) 34-38.

[111] Y. Guo, J. Li, S. Dong, Sens. Actuat. B 160 (2011) 295-300.

[112] Q.-L.Sheng, J.-B. Zheng, X.D. Shang-Guan, W.-H. Lin, Y.-Y Li, R.-X. Liu, Electrochim. Acta 55 (2010) 3185-3191.

[113] H. Hong, J. Porous Mat. 13 (2006) 393-397.

[114] F. Arifuku, K. Mori, T. Muratani, H. Kurihara, Bull. Chem. Soc. Jpn. 65 (1992) 1491-1495.

[115] H. Iken, L. Etcheverry, A. Bergel, R. Basseguy, Electrochim. Acta 54 (2008) 60-65

[116] R. Jiang, D.T. Tran, J.P. McClure, D. Chu, Electrochim. Acta 75 (2012) 185-190.

[117] J.B. Xu, T.S. Zhao, L. Zeng, Int. J. Hydrogen. Energy 37 (2012) 15976-15982.

[118] Z. X. Liang, H. Y. Song, S. J. Liao, J. Phys. Chem. C 115 (2011) 2604-2610.

[119] P.-B. Xi, Z.-X. Liang, S.-J. Liao, Int. J. hydrogen energy 37 (2012) 4606-4611.

[120] N. Zheng, Y. Zen, P.G. Osbore, Y. Li, W. Chang, Z. Wang, J. Appl. Electrochem. 32 (2002) 129-133.

[121] P.-J. Wei, G.-Q. Yu, Y. Naruta, J.-G. Liu, Angew. Chem., Int. Ed. 53 (2014) 6659-6663.

[122] L. Liu, F. Zhao, F. Ma, L. Zhang, S.Yang, N. Xia, Biosens. Bioelectr. 49 (2013) 231-235.

[123] J. Collman, R. Boulatov, Angew. Chem. Int. Ed. 41 (2002) 3487-3489.

[124] M.T. de Groot, M. Merkx, A.H. Wonders, M.T. M. Koper, J. Am. Chem. Soc.127 (2005) 7579-7586.

[125] J. Chen, U. Wollenberger, F. Lisdat, B. Ge, F. W. Scheller, Sens. Actuators B 70 (2000) 115-120.

[126] B. Duong, R. Arechabaleta, N.J. Tao, J. Electroanal. Chem. 447 (1998) 63-69.

[127] R.-I. S.-van Stadena, I. Moldoveanu, J. F. van Stadena , J. Neuro. Meth. 229 (2014) 1-7.

[128] C.G. Nan, Z.Z. Fena, W.X. Li, D.J. Ping, C.H. Qin, Anal. Chim. Acta 452 (2002) 245.

[129] T. G. Traylor, S. Tsuchiya, D. Campbell, M. Mitchell, D. Stynes, N. Koga, J. Am. Chem. Soc. 107 (1985) 604-614.

[130] J.S. Olson, R.F. Eich, L.P. Smith, J.J. Warren, B.C. Knowles, Artif. Cell. Blood Subst. Immobl. Biotech. 25 (1997) 227-241.

[131] K.J. Aoki, W. Li, J. Chen, T. Nishiumi, J. Electroanal. Chem. 713 (2014) 131-135.

[132] K. Aoki, K. Tokuda, H. Matsuda, J. Electroanal. Chem. 199 (1986) 69-79.

[133] H. Zhang, K. Aoki, J. Chen, T. Nishiumi, H. Toda, E. Torita, Electroanalysis, 23 (2011) 947-952.

[134] K. Aoki, Electroanalysis, 17 (2005) 1379-1383.

[135] P. Han, D. M. Bartels, J. Phys. Chem. 100 (1996) 5597-5602.

[136] G.C. Chu, K. Katakura, X. Zhang, T. Yoshida, M. I.-Saito, J. Biol. Chem. 274 (1999) 21319-21325.

[137] T. Komatsu, Y. Matsukawa, E. Tsuchida, Bioconjugate Chem. 13 (2002) 397-402.

[138] M. Couture, T.K. Das, P.-Y. Savard, Y. Ouellet, J.B. Wittenberg, B.A. Wittenberg, D.L. Rousseau, M. Guertin, Eur. J. Biochem. 267 (2000) 4770-4780.

[139] T. Komatsu, N. Ohmichi, P.A. Zunszain, S. Curry, E. Tsuchida, J. Am. Chem. Soc. 126 (2004) 14304-14305.

[140] H. Durliat, M. Comtat, J. Biol. Chem. 262 (1987) 11497-11500.